Title: Resistance to EGFR inhibitors in lung cancer occurs through horizontal transfer and is associated with increased caveolins expression

Authors: Susana Junqueira-Neto[1,2,3], Ana R. Oliveira[1,2,3], Joana F. Marques[1,2], Patrícia Oliveira[2], Maria G. Fernandes[1,2,3,4], Venceslau Hespanhol[1,2,3,4], Ana Barroso[5], Jorge Pinheiro[6], Conceição Souto-Moura[3,6], Bruno Cavadas[1,2], Luísa Pereira[1,2,3], Bárbara Adem[1,2], Miguel Silva[1], Sónia A. Melo[1,2,3], José L. Costa[1,2,3], José C. Machado[1,2,3,*]

Affiliations:

[1] i3S Instituto de Investigação e Inovação em Saúde, University of Porto; 4200-135 Porto, Portugal

[2]IPATIMUP Institute of Molecular Pathology and Immunology, University of Porto; 4200-135 Porto, Portugal

[3]FMUP Faculty of Medicine, University of Porto; 4200-319 Porto, Portugal

[4]Pulmonology Department, Centro Hospitalar Universitário de São João; 4200-319 Porto, Portugal

[5]Thoracic Tumors Multidisciplinary Unit, Pulmonology Department, Vila Nova de Gaia-Espinho Hospital Center; 4434-502 Vila Nova de Gaia, Portugal

[6]Pathology Department, Centro Hospitalar Universitário de São João; 4200-319 Porto, Portugal

*Corresponding author. Email: josem@ipatimup.pt

Abstract:

Resistance to treatment is a major clinical problem and a major cause of cancer-related deaths. Understanding the biological basis of resistance acquisition is of utmost importance to improve the clinical management of cancer patients. NGS analysis of human lung cancer (LC) tumors from patients that relapsed after treatment with EGFR-tyrosine kinase inhibitors (TKI), revealed that the p.T790M resistance mutation is not present in all the relapsing tumor cells, suggesting that LC cells can become resistant even if not carrying the p.T790M mutation. Using in vitro treatments with conditioned medium (CM) and in vivo co-inoculation experiments, we show that LC cells sensitive to EGFR-TKIs (S cells) acquire resistance faster when treated with CM from LC cells resistant to EGFR-TKIs (R cells) or when co-inoculated with R cells in opposite flanks of the same animal. Importantly, we show that acquisition of resistance is not due to the emergence of subpopulations of cancer cells with new resistance mutations. Using transcriptomics, we show that acquisition of resistance is associated with upregulation of genes involved in endocytosis, namely caveolins CAV1 and CAV2. These findings were validated in human clinical samples, where an increase in CAV1 and CAV2 expression was associated with tumor relapse after treatment with EGFR-TKIs. Our results suggest that acquisition of resistance to targeted therapies results from the combined effect of selection of cells harboring specific resistance mutations and horizontal transfer of the resistance phenotype. These findings may pave the way to bring intercellular communication into the realm of cancer treatment.

One Sentence Summary: Resistance to EGFR inhibitors is transferred horizontally between lung cancer cells and is associated with gain of expression of caveolins.

Main Text:

INTRODUCTION

Targeted cancer therapies block specific signalling pathways implicated in proliferation and survival of cancer cells *(1, 2)*. Despite increasing progression-free and overall survival of cancer patients, resistance to these drugs is almost universally observed *(3)*. Thus, acquired resistance to therapy is a major clinical problem and a cause of therapy failure *(4)*. Acquisition of resistance to targeted therapies is currently explained by the selective accumulation of cancer cells carrying resistance-conferring mutations *(5, 6)*. However, data on record sustain that cell division and selection cannot by itself explain the speed at which a tumour becomes clinically resistant *(7, 8)*. A study about disease progression of a melanoma patient with the BRAF p.V600E mutation is a paradigmatic example *(9)*. Furthermore, clinical data suggests that in lung cancer (LC) patients who relapse after EGFR tyrosine kinase inhibitor (TKI) treatment, cells that carry and cells that do not carry a specific resistance-conferring mutation may coexist in a treatment-resistant tumour *(10, 11)*. Hence, acquisition of resistance to targeted therapies may be influenced by mechanisms of horizontal transfer, complementing a vertical transfer model entirely dependent on cell division and selection of cells carrying resistance mutations.

Lung cancer is a prototypical model of successful use of targeted therapies, where EGFR kinase domain mutations hyperactivate and confer dependency on the EGFR oncogenic pathway for cell survival *(12, 13)*. Treatment of EGFR-mutant LC with EGFR-TKIs leads to successful clinical response in many patients *(14, 15)*. Despite initial benefit, disease progression typically develops after 9-12 months of treatment, because of the recurrent EGFR mutation p.T790M in 50-60% of cases *(16-18)*. The p.T790M mutation increases the affinity of EGFR to adenosine triphosphate, relative to its affinity to TKIs *(19)*. Resistance to EGFR-TKI therapy may also be achieved through

mutations in other genes, such as MET and ERBB2 *(20, 21)*, showing that therapy resistance does not depend solely on interference with drug activity, but may elapse also from alternative cell signalling cues. Therefore, LC constitutes a prime model to address the issue of resistance acquisition to targeted therapies, given that both sensitivity and resistance-conferring mechanisms have been identified.

We show that LC cells that do not carry known EGFR-TKI resistance mutations, acquire resistance to erlotinib faster when in the presence of LC cells that carry the p.T790M EGFR mutation. We also show that acquisition of resistance is associated with increased expression of the endocytosis associated proteins CAV1 and CAV2. Our study provides novel insight on how therapy resistance becomes a predominant phenotype in cancer and shows that widespread expression of a therapy resistance phenotype is not strictly dependent on division and selection of subpopulations of cancer cells carrying resistance triggering mutations.

RESULTS

Human lung cancers present the p.T790M resistance mutation only in a fraction of the relapsing tumour cells

Studies that characterize the EGFR sensitizing and resistance mutations *(10, 11)*, show that in some patients the allele frequency (AF) of the initial sensitizing mutation is higher than that of the resistance-conferring mutation. This suggests the resistance mutation is present only in a fraction of the relapsing tumour cells. Because this had never been studied in a systematic way, we used an NGS panel to analyse a series of 28 samples, including 14 liquid and 14 tissue biopsies (table 1), from LC patients who relapsed after EGFR-TKI treatment and where the p.T790M resistance mutation was detected.

The AF of the initial sensitizing EGFR mutation was always higher than that of the p.T790M mutation in the relapsing tumours, except for one case (table 1 and Fig. S1, $P<0.0001$). On average, the AF of the initial mutation was 3.2-fold higher than that of the p.T790M mutation, irrespective of the sample being a liquid or tissue biopsy and irrespective of the type of initial EGFR mutation, namely being a point mutation or an indel, which could affect read counting and comparison using NGS. No additional EGFR-TKI resistance mutations in any of the genes analysed were detected in these cases, excluding co-occurrence of resistance mutations as the cause for p.T790M-independent resistance. Likewise, no CNVs in EGFR were detected, excluding ploidy as the cause for observed differences in AF.

The fact that in human LC we frequently observe a lower AF for the p.T790M mutation in comparison with the sensitizing mutation in the same tumour, suggests that a fraction of the cancer cells “borrow” their resistance phenotype from cells that carry the p.T790M mutation. Our results

suggest that the fraction of cancer cells that do not carry the resistance mutation may be higher than 90% in some tumors (table 1).

Resistant cells accelerate *in vitro* acquisition of resistance by sensitive cells to EGFR-TKI

Since cancer cells can display an EGFR-TKI resistant phenotype without necessarily carrying a resistance mutation, we assessed whether resistant cells could influence acquisition of resistance to EGFR-TKI by sensitive cells *in vitro*. We used the erlotinib-sensitive LC cell line HCC827 (S cells) that harbours the sensitizing EGFR p.E746-A750del mutation, and the erlotinib-resistant LC cell line H1975 (R cells) that harbours both a sensitizing and a resistance mutation (EGFR p.L858R and p.T790M, respectively).

S cells treated with CM from R cells (Fig. 1A) achieved resistance faster in comparison to non-treated S cells (90±3 vs. 120±5 days, P=0.0009, Fig. 1B). Follow-up of S cells that acquired resistance and were further kept under erlotinib treatment only, shows that once the resistance phenotype is acquired, cells maintained a stable resistance phenotype until we stopped follow-up at 55 days.

Genetic analysis of DNA from S cells revealed that the p.T790M mutation, present in R cells, could not be detected in S cell cultures, confirming that no cell contamination occurred, and suggesting that acquisition of resistance to erlotinib in S cells is not strictly dependent on the presence of the p.T790M mutation (Fig. 1C).

Resistant cells accelerate *in vivo* acquisition of resistance by sensitive cells to EGFR-TKI

To evaluate whether R cells could influence acquisition of resistance to EGFR-TKI by S cells *in vivo*, we used a strategy of single (SI) or dual inoculation (DI) of LC cells in Rag2-/-;IL2rg-/-

immunodeficient mice (Fig. 2A). Our results show that S tumours in DI (S and R cells) mice acquire resistance significantly faster in comparison to SI (S cells only) mice (78±5 vs. 132±16 days, P=0.0006, Fig. 2B and 2C), which is reflected in a significant decrease in progression-free survival in the DI group (Fig. 2D, P=0.001). S tumours with acquired resistance to erlotinib were transplanted into new mice for two passages, always under erlotinib treatment, and maintained the ability to grow (Fig. 2E), reinforcing the *in vitro* observation that acquisition of resistance results in a stable phenotype.

To discard the possibility that migrating R cells could explain the acquisition of resistance to erlotinib in S tumors, we performed genetic analysis. Short tandem repeat (STR) profiling of S and R cells, and of S tumours from DI animals showed a perfect overlap between the profile of S tumours and S cells (Fig. 2F). To maximize the sensitivity of detection of potential migrating R cells, we also performed digital PCR for the TP53 p.R273H mutation that is present in R cells with an AF of 100% and could not detect it in S tumours (Fig. 2G). Histology analysis of R and S tumours also shows distinct morphological patterns compatible with distinct cellular origin of the tumours (Fig. S2).

Using NGS, we identified the EGFR p.E746_A750del mutation in every S tumour from DI animals with an allelic frequency (AF) similar to that of the parental S cell line (≈90%; table S1). In contrast, the p.T790M mutation is detected only in 6 out of 20 tumours and always with very low AF (≈0.1%). These results were confirmed by dPCR (Fig. 3A) and corroborate the *in vitro* observation that acquisition of resistance to erlotinib in S tumors is not dependent on the presence of the p.T790M mutation. The vestigial AF of p.T790M is most likely the result of circulating cfDNA derived from R cells growing in the opposite flank of the mice since we could not detect the p.T790M mutation in any of the S tumours from SI animals (table S1). To verify this, we

146 analyzed liquid biopsies from mice where R cells had been inoculated and confirmed that the
147 p.T790M mutation can indeed be detected in circulating cfDNA (Fig. 3B).
148 To verify whether other mutations that confer resistance to EGFR-TKIs were present in resistant
149 tumours, we used an NGS panel encompassing all known resistance mutations, including point
150 mutations in EGFR, KRAS, NRAS, BRAF and PIK3CA, and CNVs in HER2, MET and BRAF.
151 No additional point mutations were identified. Interestingly, in S tumours from SI animals we
152 identified HER2 or MET amplification in 70% of the cases (6 and 1, respectively), indicating that
153 mutation-driven resistance is a prevalent mechanism in these tumours (Fig. 3C). However, in S
154 tumours from DI animals, only MET amplification was found and only in two cases (10%, Fig.
155 3C). These results suggest that mutation-driven resistance, through the EGFR p.T790M or any
156 other known EGFR-TKI resistance mutation, is not prevalent in S tumours that acquire resistance
157 to erlotinib in DI mice.
158
159 **Caveolins are overexpressed in tumours from DI animals that acquire resistance to EGFR-**
160 **TKI**
161 Since the presence of resistance mutations does not seem to be a pre-requisite for acquisition of
162 resistance to erlotinib in S tumors from DI animals, we sought to identify what differentiates S
163 tumours growing in the presence or absence of R tumours. We used RNA-Seq to identify
164 differentially expressed genes in S tumours not treated with erlotinib and S tumors from DI animals
165 treated with erlotinib. In other words, we compared erlotinib-resistant S tumors (ERS) to erlotinib-
166 sensitive S tumors (ESS). Differentially expressed genes in ERS and ESS tumours were also
167 compared with the expression profile of R tumours under the assumption that genes relevant to

explain resistance to erlotinib in this specific biological context should be shared between ERS and R cells.

Transcriptome analysis showed that ERS tumours cluster together and are significantly different from ESS tumours (Fig. 4A). Out of the 2642 differentially expressed genes (FDR P<0.05), we represented the top 10 differentially expressed genes (Fig. 4B). Using a gene ontology approach, we observed that endocytosis was the KEGG pathway with the highest number of differentially expressed genes detected (Fig. 4C, 55 genes, P=2.46E-0.3). Within the endocytosis pathway, CAV1 and CAV2 were the most significantly overexpressed genes in ERS tumours in comparison with ESS tumours (CAV1: fold change=7.7x, FDR P=1.23E-0.5; and CAV2: fold change=4.2x, FDR P=4.9E-0.7, Fig. 4D and Fig. S3).

Expression analysis through qPCR validated that CAV1 and CAV2 are overexpressed both in ERS tumours and R tumours, when compared with ESS tumours (Fig. 5A). The same was observed for protein immunohistochemistry expression, with both ERS tumours and R tumours showing strong CAV1 and CAV2 expression in tumours cells, whereas in ESS tumours CAV1 and CAV2 expression showed weak and focal expression in tumours cells (Fig. 5B and C).

Caveolins are overexpressed in human lung cancers that progress after EGFR-TKI treatment

To validate our findings, we compared the immunohistochemical expression of CAV1 and CAV2 in human LC before and after treatment with erlotinib. We selected fifteen cases of LC harbouring sensitizing EGFR mutations and treated first-line with erlotinib, in which the p.T790M EGFR mutation was detected as the resistance mechanism, and for which treatment-naïve and post-progression tissue biopsies were available. CAV1 and CAV2 protein expression was mainly

localized in the cell membrane of tumour cells, although some cytoplasmic staining could be detected as well. Staining in the endothelium and connective tissue was also detected (Fig. 6A). Out of the 15 pairs of samples analysed for CAV1 expression, 80% were negative before treatment and 20% showed moderate expression (Fig 6B). CAV2 expression could only be analysed in 10 pairs of cases due to lack of material. 75% of the cases were negative before treatment, 17% displayed moderate expression and 8% had strong expression (Fig 6B). From pre-treatment to post-progression samples, we observed a significant increase (P=0.007) in CAV1 expression in 67% of the cases: from no to moderate expression in 5 cases; from no to strong expression in 3 cases; and from moderate to strong expression in 2 cases (Fig. 6B, table S2). A significant increase (P=0.04) in CAV2 expression was observed in 60% of the cases: from no to moderate expression in 3 cases; from no to strong expression in 1 case; and from moderate to strong expression in 2 cases (Fig. 6B, table S2).

204 **Table 1.** Allele frequencies determined by NGS in LC samples after disease progression.

Patient	Biopsy type	EGFR sensitizing mutation	AF sensitizing mutation	AF p.T790M mutation	Fraction
1	Liquid	c.2239_2256del; p.Leu747_Ser752del	0.8%	0.3%	62.5%
2	Liquid	c.2573T>G; p.Leu858Arg	65%	29%	55.4%
3	Liquid	c.2235_2249del; p.Glu746_Ala750del	13%	3%	76.9%
4	Liquid	c.2235_2249del; p.Glu746_Ala750del	3%	0.3%	90.0%
5	Liquid	c.2573T>G; p.Leu858Arg	19%	3%	84.2%
6	Liquid	c.2573T>G; p.Leu858Arg	11%	7%	36.4%
7	Liquid	c.2235_2249del; p.Glu746_Ala750del	3%	1.8%	40.0%
8	Liquid	c.2236_2250del; p.Glu746_Ala750del	2.6%	0.8%	69.2%
9	Liquid	c.2236_2250del; p.Glu746_Ala750del	11.9%	1.7%	85.7%
10	Liquid	c.2573T>G; p.Leu858Arg	27.6%	1%	96.4%
11	Liquid	c.2240_2257del; p.Leu747_Pro753delinsSer	2%	0.6%	70.0%
12	Liquid	c.2235_2249del; p.Glu746_Ala750del	11%	4.2%	61.8%
13	Liquid	c.2240_2257del; p.Leu747_Pro753delInsSer	1.8%	1.9%	0%
14	Liquid	c.2235_2249del; p.Glu746_Ala750del	82%	47%	42.7%
15	Tissue	c.2238_2261delinsGCAAC; p.Leu747Glnfs*13	61%	10%	83.6%
16	Tissue	c.2573T>G; p.Leu858Arg	20%	6%	70.0%
17	Tissue	c.2240_2257del; p.Leu747_Pro753delInsSer	24%	18%	25.0%
18	Tissue	c.2235_2249del; p.Glu746_Ala750del	29%	7%	75.9%
19	Tissue	c.2235_2249del; p.Glu746_Ala750del	40%	14%	65.0%
20	Tissue	c.2235_2249del; p.Glu746_Ala750del	84%	10%	88.1%
21	Tissue	c.2573T>G; p.Leu858Arg	53%	25%	52.8%
22	Tissue	c.2235_2249del; p.Glu746_Ala750del	31%	8%	74.2%
23	Tissue	c.2573T>G; p.Leu858Arg	26%	2%	92.3%
24	Tissue	c.2573T>G; p.Leu858Arg	41%	1%	97.6%
25	Tissue	c.2235_2249del; p.Glu746_Ala750del	45%	24%	46.7%
26	Tissue	c.2240_2257del; p.Leu747_Pro753delInsSer	15%	3%	80.0%
27	Tissue	c.2236_2250del; p.Glu746_Ala750del	60%	16%	73.3%
28	Tissue	c.2236_2250del; p.Glu746_Ala750del	14%	7%	50.0%

205 AF, allele frequency; Fraction, the fraction of cancer cells that do not carry the resistance mutation
206 as inferred by the formula (1-AF p.T790M/AF sensitizing).

207

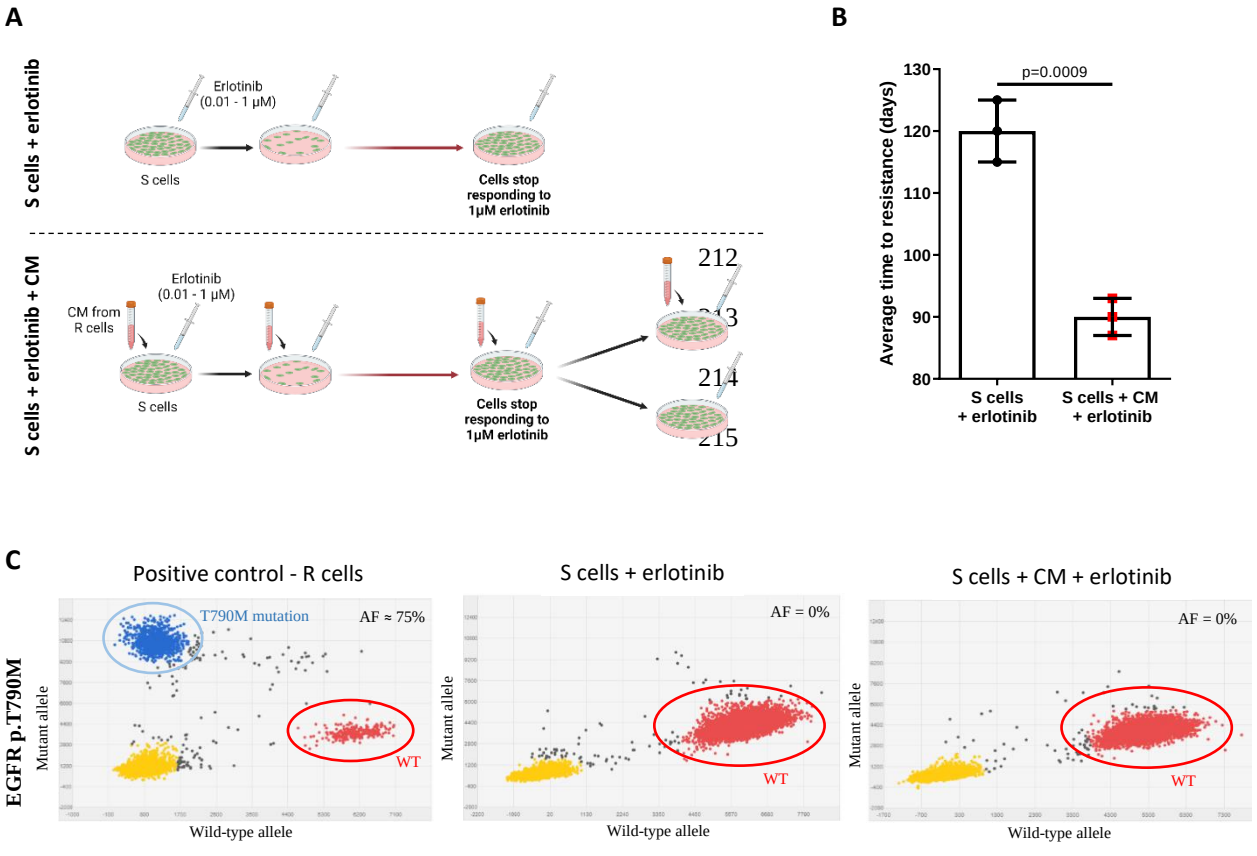

Figure 1. R cells accelerate *in vitro* acquisition of resistance to EGFR-TKI by S cells. (**A**) Experimental outline of S cells treated with conditioned media (CM) from R cells, and S cells without CM. In both experiments, S cells were treated with increasing concentrations of erlotinib (0.01-1 µM). Resistance was achieved when cells stopped responding to the treatment. CM-treated cells were further divided into two groups, one maintaining the treatment with CM and erlotinib, and the other with erlotinib only. (**B**) Comparison of the average time to resistance in days between CM-treated cells and CM-untreated cells (Mean ± SD). (**C**) Digital PCR plots for the p.T790M assay. The *EGFR* p.T790M mutation is not present in DNA from any of the CM-treated or CM-untreated cells: yellow dots represent empty wells; blue dots represent the T790M variant; red dots correspond to the wild-type sequence; and grey dots represent polyclonal wells not considered for analysis. The AF (allelic frequency) is calculated dividing the number of blue dots by the sum of blue and red dots.

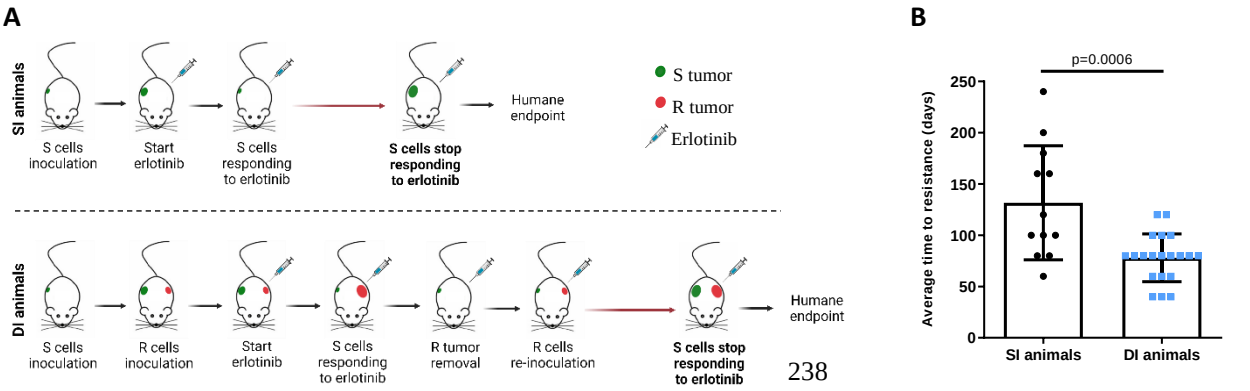

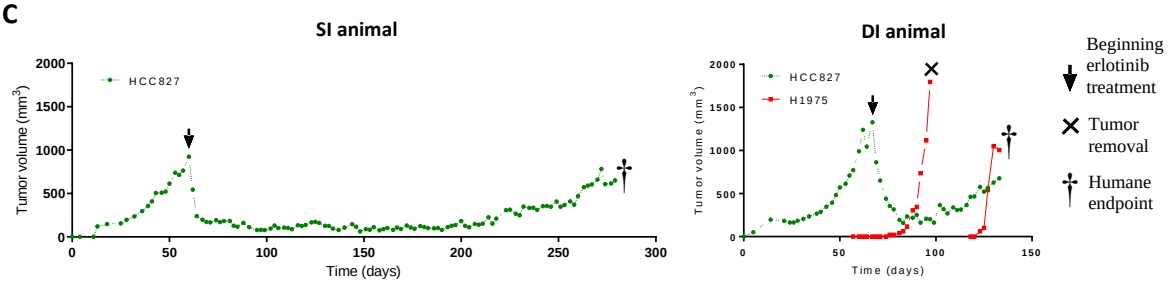

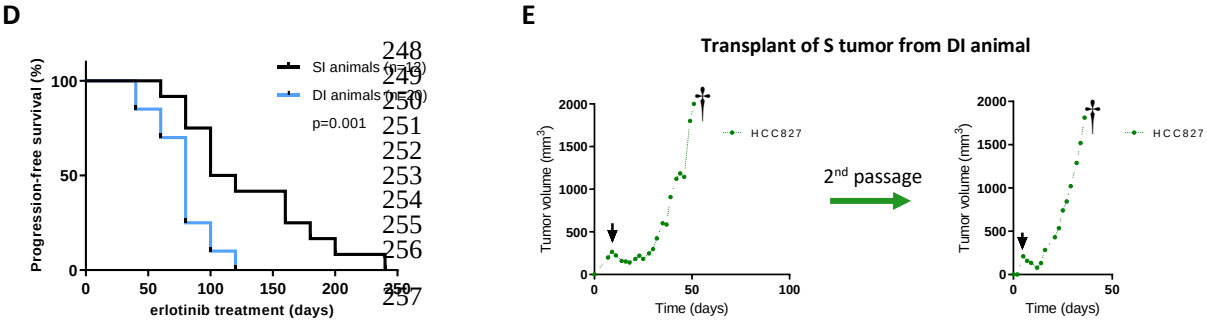

F

Short Tandem Repeat profiling																
Sample	D3S1358	TH01	D21S11	D18S51	Penta E	D5S818	D13S317	D7S820	D16S539	CSF1PO	Penta D	Amel	VWA	D8S1179	TPOX	FGA
S tumor (DI animal)	17	6	31	13	20	12	9	11-12	12	11	14	X	18	12	8	22-24
S cells	17	6	31	13	20	12	9	11-12	13	11	14	X	18	12	8	22-24
R cells	14-15	7	28	13	12	11-12	10-13	8	9-12	12	12-13	X	18	13-16	11	21

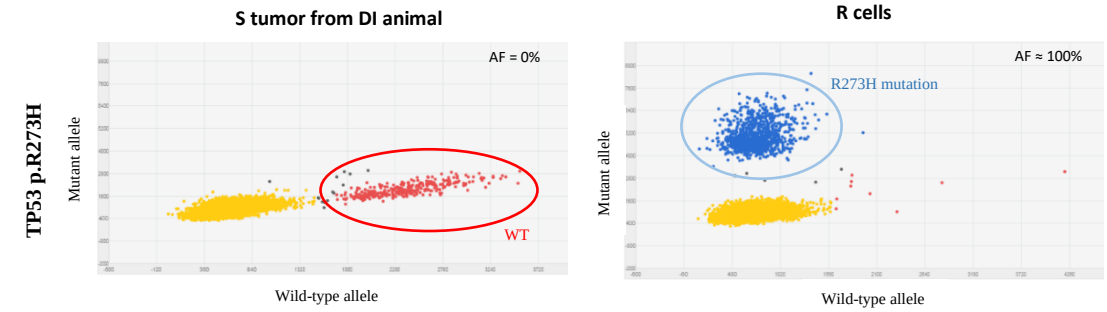

Figure 2. R cells accelerate *in vivo* acquisition of resistance to EGFR-TKI by S cells. (**A**) Experimental outline of mice engrafted with S cells inoculated in a single flank (SI animals) and mice engrafted with S and R cells inoculated in opposite flanks (DI animals) treated with erlotinib 3 times/week by oral gavage. (**B**) Comparison of the average time to relapse in days between DI and SI animals (Mean ± SD). (**C**) Tumor growth kinetics of one representative SI and one representative DI mouse, illustrating that S tumors in DI animals acquire resistance faster. (**D**) Progression-free survival curves of SI and DI animals are significantly different (P=0.001; Log-rank Mantel-Cox test). (**E**) After resistance acquisition, S tumors from DI animals were re-inoculated into new mice for two passages and erlotinib treatment was maintained during the whole experiment. (**F**) Comparison of the STR profile of S tumors from DI animals with the STR profile of S and R cells. (**G**) dPCR plots of S tumor from a DI animal negative for the *TP53* p.R273H mutation and of R cells positive for the *TP53* p.R273H mutation with 100% AF.

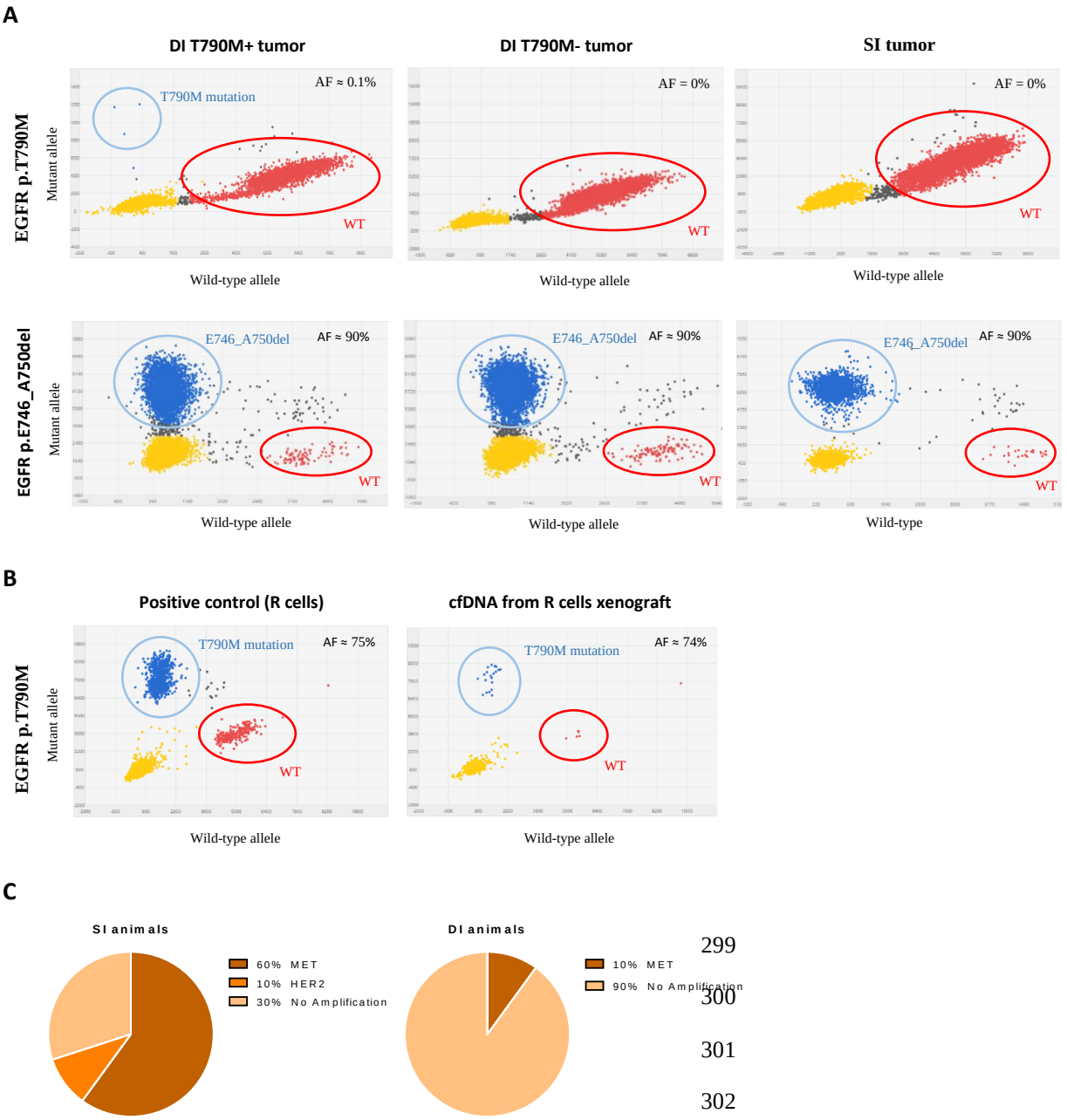

Figure 3. Detection of resistance mutations to EGFR-TKI in S tumors from SI and DI animals. (**A**) dPCR plots for *EGFR* p.T790M and *EGFR* p.E746_A750del mutations in representative examples of S tumors from SI and DI animals. S tumor from DI animal positive for *EGFR* p.T790M mutation with 0.1% AF (left panel); S tumor from DI animal negative for *EGFR* p.T790M mutation (middle panel); S tumor from SI animal negative for *EGFR* p.T790M mutation (right panel). All samples are positive for the *EGFR* p.E746_A750del mutation with ≈90% AF. (**B**) dPCR plots for the p.T790M mutation. The *EGFR* p.T790M mutation is present in the cfDNA from mice xenografted wit R cells (right panel) with an AF similar to that of the parental R cell line (left panel). (**C**) NGS data on *MET* and *HER2* gene amplification in S tumors from SI animals (left diagram) and from DI animals (right diagram).

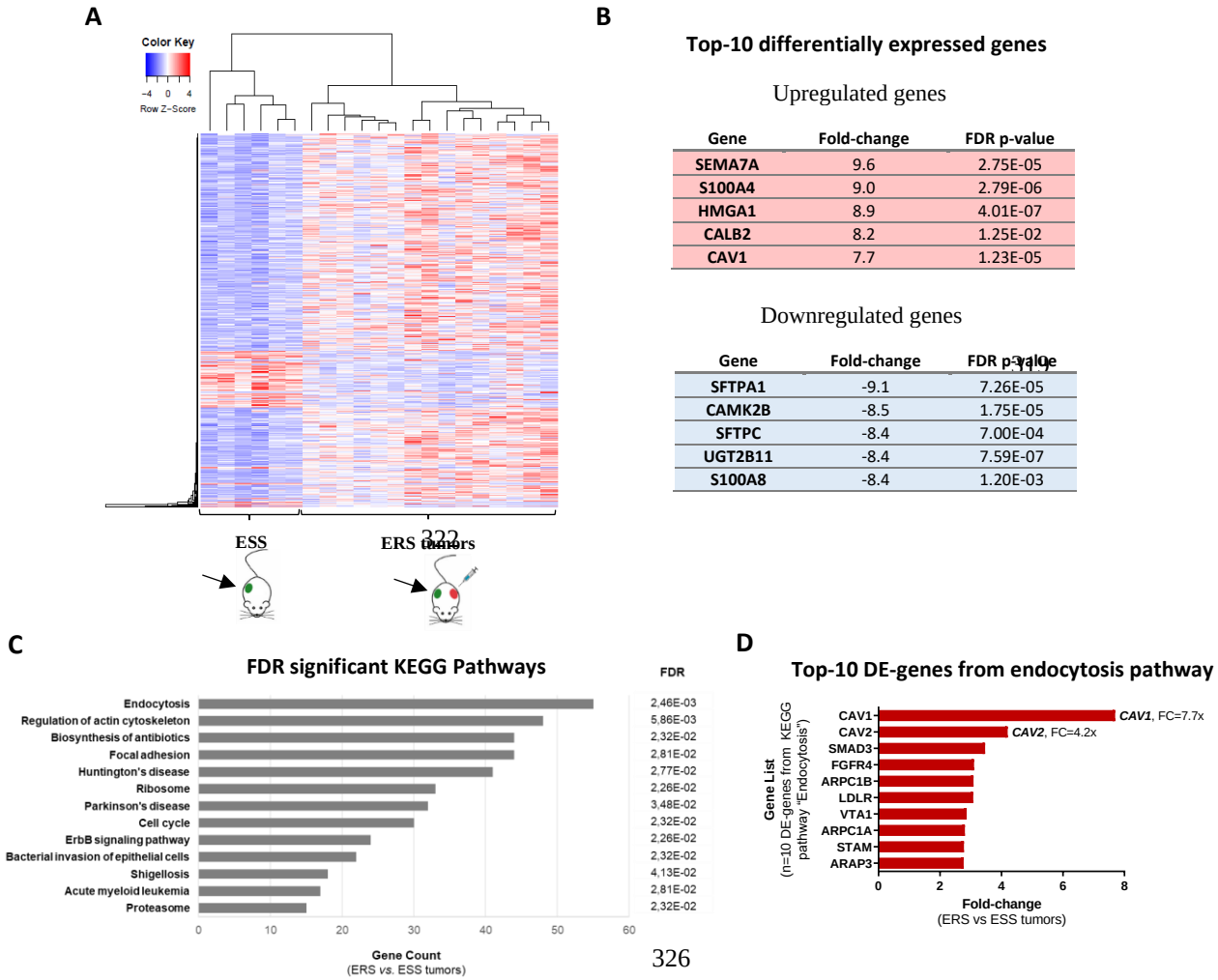

Figure 4. Identification of endocytosis as the mechanism associated with resistance acquisition in ERS tumors. (**A**) Heatmap for RNA-Seq gene expression profiles for ESS tumors versus ERS tumors. FDR p-value <0.05; 2642 differentially expressed (DE) genes. (**B**) Top-10 DE-genes between ERS and ESS tumors (top-5 upregulated genes and top-5 downregulated genes). (**C**) Gene ontology showed endocytosis KEGG pathway as the pathway with the highest number of genes detected and the best FDR p-value (55 genes, FDR *P*=2.46E-0.3). (**D**) Top-10 DE-genes between ERS and ESS tumors from the endocytosis KEGG pathway (FDR *P*<0.05). FC – fold change.

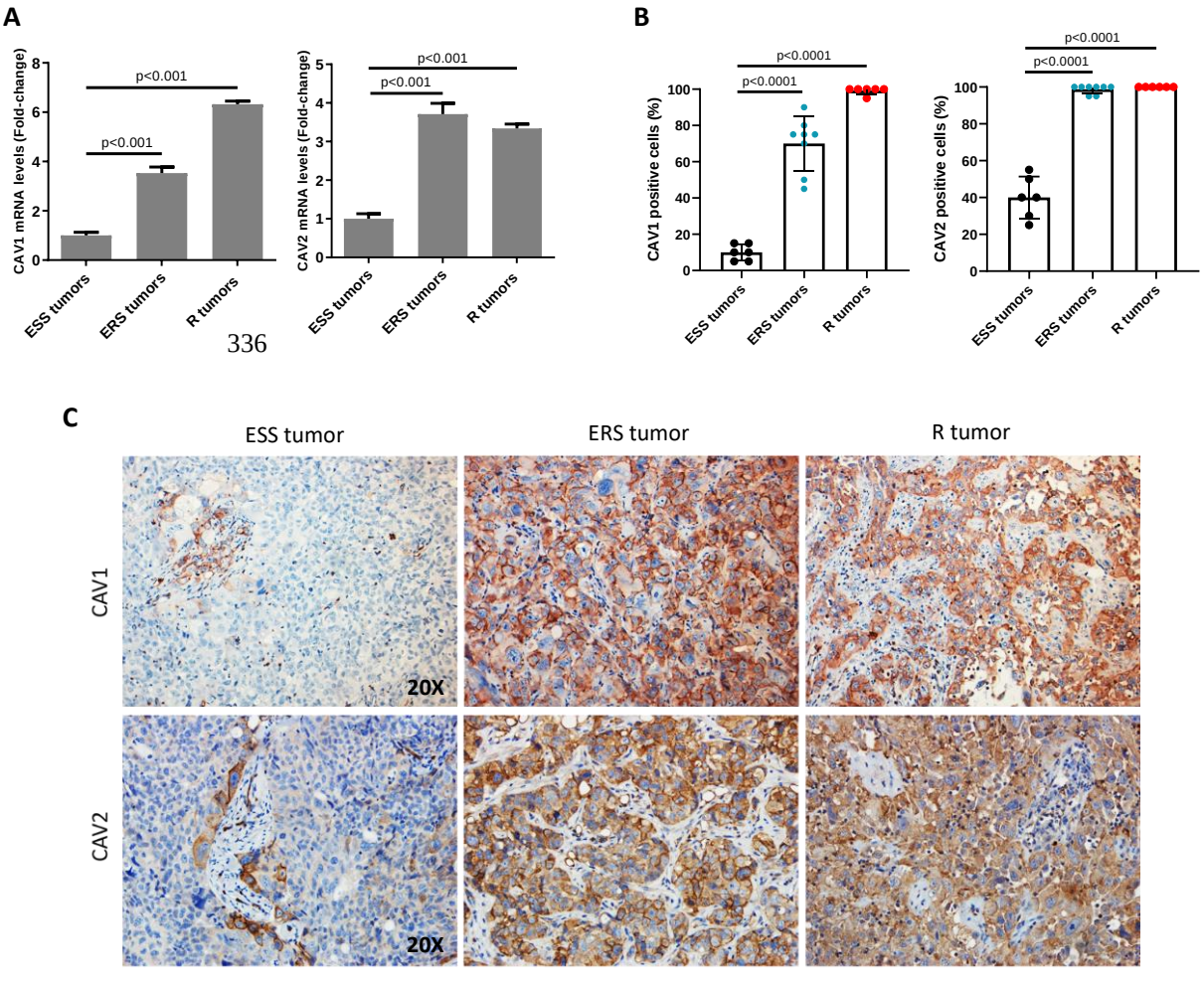

Figure 5. Validation of increased caveolins expression in ERS tumors by real time PCR and immunohistochemistry (IHC). (**A**) The bars represent the $2^{-\Delta\Delta Ct}$ as a fold-change of the *CAV1* (left) and *CAV2* (right) mRNA expression, normalized to *GUSβ* and *HPRT1*, for ESS tumors, ERS tumors and R tumors. (Mean ± SE; $P<0.001$). (**B**) Percentage of CAV1 and CAV2 protein positive cells for ESS tumors, ERS tumors and R tumors (Mean ± SD; $P<0.0001$). (**C**) CAV1 and CAV2 immunohistochemistry expression in representative examples of ESS tumors, ERS tumors and R tumors (magnification x200). ESS tumors show weak focal expression in tumor cells and staining in perivascular cells; ERS tumors and R tumors show strong and diffuse expression of caveolins in tumor cells.

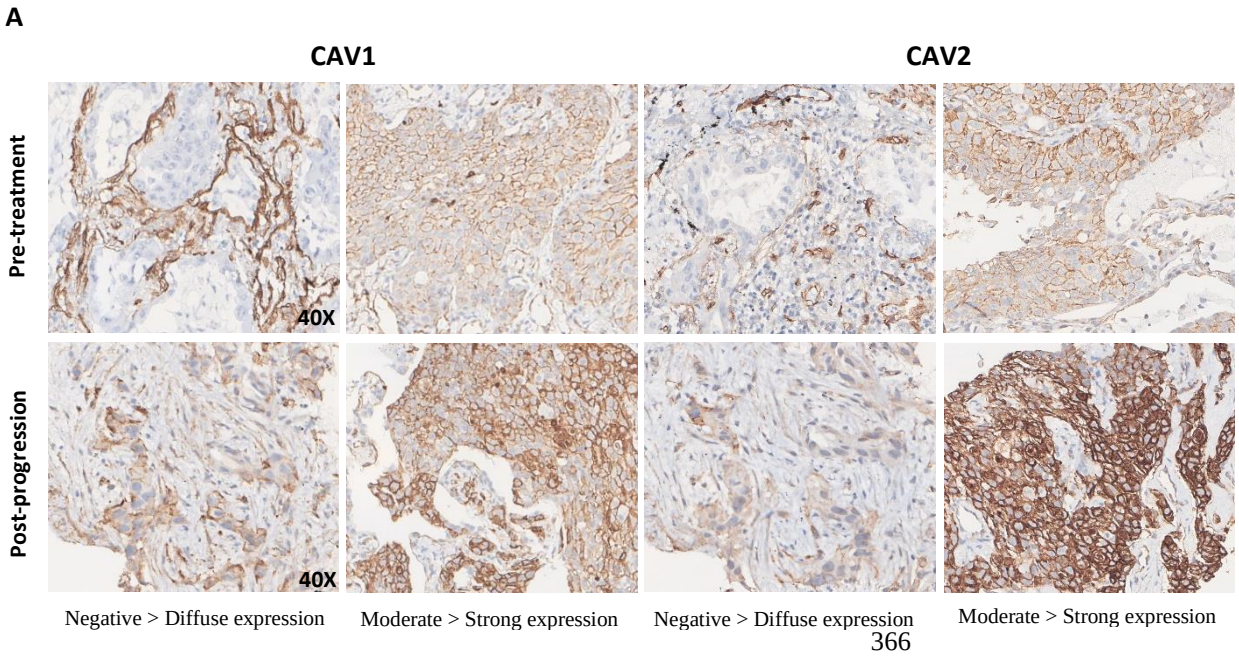

Figure 6. Increased expression of caveolins in EGFR-mutated human NSCLC after resistance acquisition to EGFR-TKI. (**A**) Microscopy images of CAV1 and CAV2 protein expression detected by immunohistochemistry in representative examples of untreated primary NSCLC (upper panel) and EGFR-TKI treated, p.T790M mutated relapsing tumors (lower panel) (magnification x400). CAV1 and CAV2 protein was mainly localized in the membrane with some cytoplasm staining in tumor cells. Endothelium and connective tissue also stained. (**B**) Percentage of pre-treatment and post-progression cases with negative, moderate, and strong expression of CAV1 and CAV2.

DISCUSSION

One of the main implications of our findings is that mutation-driven resistance to targeted therapies can be transferred among cancer cells. Both *in vitro* and *in vivo* data show that in the presence of R cells, either using CM or through dual inoculation in the same animal, S cells acquire resistance faster. In mice, this results in shorter progression-free survival. Most importantly, we show that acquisition of resistance, as observed in S cells that grow alone (SI animals), is intrinsically different from what occurs in S cells that grow in DI animals. In the former, 70% of the tumours present with known EGFR-TKI resistance-associated mutations, namely MET and ERBB2 amplification, whereas in the latter these events are rare, with 90% of the tumours showing no evidence of mutation-associated resistance mechanisms.

Our results challenge the established paradigm that resistance to targeted therapies occurs because cancer cells harbouring resistance-conferring mutations, which initially exist in small numbers, are selected, accumulate, and eventually take over the entire tumour cell population through a vertical transmission model solely reliant on cancer cell division *(5)*. Furthermore, our clinical data on the AF of sensitizing and resistance mutations shows that in LC patients who relapse after EGFR-TKI treatment, the p.T790M mutation is present only in a fraction of the relapsing tumour cells. Assuming equal ploidy for the sensitizing and resistance alleles, as suggested by NGS CNV analysis, our data indicates that the fraction of cancer cells carrying the resistance mutation corresponds to about one-third, although this proportion may vary widely. These observations, support the idea that although resistance stems from a genetic mutation, cancer cells may become resistant even though they do not carry that mutation, opening the door to a model of cell-to-cell horizontal transfer of resistance.

Horizontal transfer of phenotypes is commonly observed in bacteria, which by exchanging genetic material, gain new traits such as resistance to antibiotics *(22)*. Horizontal transfer can also take place in eukaryotes, with exogenous DNA impacting the phenotype of recipient cells via mediators such as transposons, cfDNA, or extracellular vesicles (EVs) *(22)*. However, the role of horizontal transfer in cancer is largely unknown. Our results do not support the hypothesis that acquisition of resistance in S cells "exposed" to R cells is due to genetic transfer of the p.T790M mutation. Even though the resistance phenotype is stable in S cells, as these cells maintain the capacity to grow *in vitro* and *in vivo* under treatment with erlotinib, the p.T790M mutation originating in R cells could hardly be detected in S cells. Moreover, even if we accept the remote possibility that DNA coding for the p.T790M mutation is stably incorporated into the genome of some S cells, endowing them with resistance to erlotinib, this mechanism alone could not explain the widespread resistance phenotype observed in the resulting S tumours.

We reason that the full blown and stable resistance phenotype observed in our model is triggered by the p.T790M mutation in R cells, coupled with a continuous flow of molecular information from R to S cells, and among S cells. It has been shown that EVs carry proteins, RNA transcripts and other molecular material *(23, 24)*, making it a likely candidate to explain horizontal transfer of resistance across cancer cells. In fact, EV-mediated transfer of molecules has been shown to contribute to phenotypic reprogramming and functional re-education of recipient cells *(25, 26)*. Noteworthy, it has been recently reported that exosomal transfer of wild-type EGFR protein promotes resistance to osimertinib (a third-generation EGFR-TKI drug) in LC *(27)*.

A key finding of our study is the demonstration that horizontal transfer of resistance triggers a change in the transcriptional landscape of ERS tumours. Pathway analysis showed significant changes in genes involved in endocytosis, namely overexpression of CAV1 and CAV2.

Overexpression was confirmed at the mRNA and protein level in samples from our *in vivo* model and at the protein level in clinical LC samples. The results obtained in clinical samples are especially relevant because they correspond exactly to the model of acquisition of resistance to erlotinib determined by the occurrence of the p.T790M EGFR mutation. In our series, 67% and 60% of the cases showed gain of CAV1 and CAV2 expression, respectively, comparing the pre-treatment to the post-progression samples.

Caveolins are membrane-associated proteins that play a key role in the formation of non-planar lipid rafts known as caveolae *(28)*. In turn, caveolae are important for signal transduction through their capacity to selectively concentrate proteins, such as membrane receptors, kinases, and phosphatases, thereby promoting specific molecular interactions *(29)*. Caveolins are also involved in intracellular trafficking, including endocytosis, through their localization in distinct cellular organelles and compartments *(30)*. Caveolins, namely CAV1 and CAV2, have been involved in cancer with both oncogenic and tumour suppressor properties being described *(31)*. CAV1, for instance, tends to be expressed in normal cells, downregulated during neoplastic transformation and first stages of tumour progression, and re-expressed in late stages associated with treatment resistance and metastasis *(31)*.

In LC, increased CAV1 expression was associated with gemcitabine resistance *(32)*, and poor prognosis *(33, 34)*. Caveolins have also been demonstrated to modulate EGFR activity in cancer cells. CAV2 was shown to promote the growth of renal cell carcinoma cells through EGFR signalling *(35)*. *In vitro*, CAV1 was shown to increase LC cell proliferation, migration, and invasion through EGFR phosphorylation *(36)*. Most importantly, silencing of CAV1 in LC cells led to enhanced sensitivity to EGFR-TKI drugs by down-regulating phosphorylation of EGFR *(37)*, directly supporting our contention that the acquisition of resistance to erlotinib is associated

with increased CAV1 and CAV2 expression. The precise mechanism linking caveolins to EGFR-TKI resistance is not known, however, published evidence indicates it is likely to involve increased EGFR signalling and increased endocytosis. There is evidence that such increase in endocytosis is accompanied by overexpression and nuclear translocation of both EGFR and other membrane receptors *(30, 38)*, which in turn may provide survival signals to overcome the inhibitory effect of EGFR-TKI drugs.

In conclusion, our results suggest that the EGFR-TKI resistance phenotype can be transferred from resistant to sensitive cells both *in vivo* and *in vitro*, resulting in reprogramming of the cells that acquire resistance. Our findings point out a key role for endocytosis, coupled with caveolae-associated regulation of signaling and intracellular trafficking, in the acquisition of resistance to targeted therapies in cancer. Even though our study does not elucidate how transfer of resistance occurs, or the specific mechanism linking caveolins with EGFR-TKI resistance, we present a strong case to challenge the current paradigm of cell division and selection as the sole mechanism underlying transmission of mutation-driven resistance to targeted therapies. In addition, our study provides a proof of concept to trigger further research on whether these results can be applied to other models of targeted therapy and mutation-driven acquisition of resistance in cancer.

MATERIALS AND METHODS

Human samples

Samples from patients with advanced lung adenocarcinoma (unresectable stages IIIB and IV) were obtained from the Pulmonology Departments of Centro Hospitalar de São João and Centro Hospitalar de Vila Nova de Gaia/Espinho. Pre- and post-EGFR-TKI treatment tumour tissue biopsies from 15 LC patients were used for immunohistochemistry. Post-EGFR-TKI treatment liquid and tissue biopsies from LC patients (14+14) were selected for NGS analysis. Blood samples were collected in K_2EDTA tubes (BD Vacutainer® PPT™ Plasma Preparation Tube, Becton Dickinson, Franklin Lakes, USA). The plasma fraction was separated from the blood cells by centrifugation at 1200xg during 10min. The collected plasma was aliquoted and stored at −80°C for cell-free DNA (cfDNA) extraction. Histology and cytology specimens were formalin-fixed and paraffin-embedded and reviewed by a pathologist.

Cell lines and cell culture

Human LC cell lines HCC827 (ATCC Cat# CRL-2868™) and H1975 (ATCC Cat# CRL-5908™) were cultured in RPMI-1640 medium [GIBCO, USA], supplemented with 10% (v/v) foetal bovine serum (FBS) [GIBCO, USA], 100 U/mL penicillin and 100µg/mL Streptomycin [GIBCO, USA]. Cells were kept at 5% CO_2 and 37°C in a humidified atmosphere. Cells were tested for mycoplasma during our study and STR profiled.

Conditioned medium experiment

LC cells sensitive to the EGFR-TKI (S cells) were seeded in a 6-well plate, $2.5x10^5$ cells/well. After 24h, medium from LC cells resistant to the EGFR-TKI (R cells) was collected, centrifuged

at 4,000rpm for 10min and filtered using 0.45μm filter, before being added to S cells, together with 0.01μM EGFR-TKI. The EGFR-TKI included in this study was erlotinib [LC Laboratories, Woburn, MA, USA]. Erlotinib stock solution was prepared in 0.5% [wt/vol] methylcellulose [Sigma-Aldrich®, St. Louis, MO, USA] and 0.4% [vol/vol] Tween-80 [Sigma-Aldrich®, St. Louis, MO, USA] solution. Experiments were performed with three replicates per condition.

LC xenograft model

S cells (5×10^6) and R cells (1×10^5) were subcutaneously injected into the dorsal flank of 8-12-weeks-old immunodeficient C57BL/6 *Rag2*$^{-/-}$*;Il2rg*$^{-/-}$ mice. We engrafted S cells in one flank and once tumours reached a size ≈800mm^3, R cells were engrafted in the opposite flank. When the S tumours reached ≈1000mm^3, erlotinib was administered (3 times/week, oral gavage, 25mg/kg). Due to rapid growth of the R tumours, surgery was performed to remove these tumours when it reached 1500mm^3 of size and after 1-2 weeks of recovery, mice were again engrafted with R cells. This procedure allowed to follow-up S cell tumours for longer periods of time until acquisition of resistance to erlotinib. In both groups, animals were sacrificed at humane endpoint. A set of animals were engrafted with S cells in a single flank and used as control. Tumour size was measured with callipers every other day and tumour volume calculated by the formula length×width^2/2. Disease progression was defined as an increase of at least 75% in volume with respect to the minimum tumour volume after treatment. At humane endpoint, mice were euthanized, and tumours dissected and immersed in 10% formalin, for histological and molecular analysis.

DNA extraction

514 DNA from cells was extracted using DNeasy® Blood & Tissue kit [QIAGEN, Hilden, Germany],
515 according to manufacturer's instructions. Tumour samples from mice and tissue biopsies from
516 patients were cut in 10µm sections using the Microm HM 335 E paraffin microtome [GMI,
517 Ramsey, MN, USA] and 3 sections of each sample were collected. DNA and RNA extraction were
518 performed using MagMAX^{TM} FFPE DNA/RNA Ultra Kit [Thermo Fisher Scientific, Waltham,
519 MA, USA], according to manufacturer's instructions.
520 cfDNA from plasma patients was extracted using MagMAX Cell-Free DNA Isolation kit [Applied
521 Biosystems, Life technologies, Waltham, MA, USA], according to manufacturer's instructions.
522 Fragment distribution and concentration of DNA from plasma was evaluated using 2200
523 TapeStation [Agilent Technologies, Santa Clara, CA, USA], according to manufacturer's
524 instructions. The results were analysed with the TapeStation Analysis Software [Invitrogen, Life
525 technologies, Waltham, MA, USA]. All plasma DNA quantifications were normalized for volume
526 of plasma collected [cfDNA concentration (ng/mL of plasma) = cfDNA quantification (ng/µL) x
527 elution volume (µL) / plasma volume (mL)].
528 DNA and RNA concentration were determined using Qubit® 2.0 Fluorometer [Invitrogen, Life
529 technologies, Waltham, MA, USA], double stranded DNA high sensitivity (HS) or RNA HS assay,
530 according to manufacturer's instructions.
531

532 **DNA fingerprinting**

533 DNA from cells was amplified through PCR with primers for the following locus: Penta E,
534 D18S51, D21S11, THO1, D3S1358, FGA, TPOX, D81179, vWA, Amelogenin, Penta D,
535 CSF1PO, D16S539, D7S820, D14s317 and D5S818 with the Powerplex 16 HS system, that allows
536 the co-amplification and simultaneous detection of the 16 described loci. The amplified fragments

were then detected with capillary electrophoresis using the 3500 Genetic Analyser sequencer [Applied Biosystems] and the genotypes were assigned with the GeneMapper v5.0 [Applied Biosystems].

Next Generation Sequencing (NGS)

NGS libraries were prepared using the Oncomine™ Lung cfDNA Assay for mouse xenografts and for human liquid biopsies, and the Oncomine™ Focus Assay for human tissue biopsies according to the manufacturer's instructions [Thermo Fisher Scientific, Waltham, MA, USA]. The resulting libraries were purified using Agencourt AMPure XP [Beckman Coulter] and quantified by qPCR using the Ion Library TaqMan® Quantitation Kit [Thermo Fisher Scientific, Waltham, MA, USA], according with the manufacturer instructions. The quantified stock libraries were then diluted to 50pM, pooled and loaded onto Ion 530™ or 540™ chips using Ion Chef™ for templating [Thermo Fisher Scientific, Waltham, MA, USA] and the loaded chips were then sequenced in a S5XL sequencer. The sequencing quality was assessed through the coverage analysis plugin and the samples were analysed with Ion Reporter 5.6. Raw data was processed automatically on the Torrent Server™ and aligned to the reference hg19 genome.

Digital PCR

TaqMan Mutation Detection Assays [Thermo Fisher Scientific, Waltham, MA, USA] were used on a Quantstudio 3D digital PCR system [Thermo Fisher Scientific, Waltham, MA, USA] to confirm variants with low allelic frequencies. This approach was used to detect specific alterations, with specific probes for each mutation, namely the Hs000000029_rm (for *EGFR* p.T790M mutation), Hs000000026_rm (for *EGFR* p.L858R mutation), Hs000000027_rm (for *EGFR*

p.E746-A750 deletion) and Hs00001004_mu (for TP53 p.R273H mutation). The results were analysed with QuantStudio™ 3D AnalysisSuite™ Software.

RNA-Seq

The integrity and quality of RNA was analysed using the Agilent 2100 Bioanalyzer [Agilent Technologies, Santa Clara, CA, USA]. RNA was converted to cDNA using the SuperScript VILO cDNA Synthesis Kit [Thermo Fisher Scientific, Waltham, MA, USA]. cDNA was amplified and library constructed with Ion AmpliSeq Transcriptome Human Gene Expression Kit [ThermoFisher Scientific, Waltham, MA, USA]. Samples were then prepared for deep sequencing using the Ion Chef™ System [Thermo Fisher Scientific, Waltham, MA, USA], loaded into the Ion 550 Chip, and sequenced using the Ion S5 XL Sequencer [Thermo Fisher Scientific, Waltham, MA, USA]. Sequencing quality was assessed through the plug-in coverage analysis and samples were analysed on the torrent Suite™ Software [Thermo Fisher Scientific, Waltham, MA, USA]. Differentially expressed genes between groups were identified using the Transcriptome Analysis Console Software v4.0.2 [Thermo Fisher Scientific, Waltham, MA, USA] using a double threshold based on fold-change (>=1 ou <=-1) and statistical significance of the change with FDR p-value <=0.05. DAVID webtool was used to determine significantly enriched gene ontology terms and pathways.

Real time PCR

RNA was converted to cDNA using the SuperScript VILO cDNA Synthesis Kit [Thermo Fisher Scientific, Waltham, MA, USA], according to manufacturer's instructions. The reactions were carried out in a StepOnePlusTM qPCR Real-Time PCR machine, in a volume of 10µL containing 1x TaqManTM Fast Advanced Master mix [Applied Biosystems], with 1x TaqManTM Advanced

Assays probes Hs00971716_m1 and Hs00184597_m1 [Applied Biosystems] specific for the *CAV1* and *CAV2* gene, respectively, and 2.5µL cDNA. For mRNA expression normalization, two housekeeping controls were used: HPRT1 and GUSB [Applied Biosystems]. The $2^{-\Delta\Delta CT}$ method was applied to analyse the relative change in gene expression. Three technical replicates were made for each sample.

Immunohistochemistry

Tissue sections were obtained in coated slides [Thermo Scientific, Waltham, MA, USA], 3µm each section, using the Microm HM 335 E paraffin microtome [GMI, Ramsey, MN, USA] followed by incubation at 65°C for 1h. Each section was probed overnight at 4°C with an optimized concentration of the anti-CAV1 (Sigma-Aldrich®, catalog #HPA049326, 1:1000) and anti-CAV2 (Novus Biologicals, catalog #NBP2-98731, 1:500) polyclonal antibodies diluted in antibody diluent [Thermo Scientific, Waltham, MA, USA]. CAV1 and CAV2 proteins were detected by peroxidase-DAB (diaminobenzidine) chemistry using the REAL EnVision detection system kit [Dako, Glostrup, Denmark]. CAV1 and CAV2 immunoreactivity was classified as: (1) negative, when tumour cells showed complete loss of expression; (2) moderate, when less than 50% of the tumour cells showed preserved membrane expression, or, irrespective of the percentage of cells, weaker membrane staining compared with the control; or (3) strong, when more than 50% of the tumour cells showed preserved membrane expression.

Statistical analysis

All statistical analyses were performed with GraphPad Prism [GraphPad Prism, RRID:SCR_002798], SPSS Statistics V27 Release 27.0.1.0. [IBM, RRID:SCR_019096] or R

606 software package (https://www.r-project.org). The data were showed as means ± standard
607 deviation (SD) and analysed by Student's *t*-test analysis unless otherwise indicated. Log-Rank
608 (Mantel-Cox) test was used to compare progression-free survival onset between different mice
609 models. Pearson correlations between gene expressions of CAV1 and CAV2 were performed using
610 the "cor.test" package in R.
611

List of Supplementary Materials

Figs. S1 to S3.

Tables S1 and S2.

References and Notes

1. C. Sawyers, Targeted cancer therapy. *Nature* **432**, 294-297 (2004).
2. D. Gonzalez de Castro, P. A. Clarke, B. Al-Lazikani, P. Workman, Personalized cancer medicine: molecular diagnostics, predictive biomarkers, and drug resistance. *Clin Pharmacol Ther* **93**, 252-259 (2013).
3. D. R. Camidge, W. Pao, L. V. Sequist, Acquired resistance to TKIs in solid tumours: learning from lung cancer. *Nat Rev Clin Oncol* **11**, 473-481 (2014).
4. L. A. Garraway, P. A. Janne, Circumventing cancer drug resistance in the era of personalized medicine. *Cancer Discov* **2**, 214-226 (2012).
5. B. G. Blair, A. Bardelli, B. H. Park, Somatic alterations as the basis for resistance to targeted therapies. *J Pathol* **232**, 244-254 (2014).
6. C. B. Meador *et al.*, Optimizing the sequence of anti-EGFR-targeted therapy in EGFR-mutant lung cancer. *Mol Cancer Ther* **14**, 542-552 (2015).
7. N. McGranahan, C. Swanton, Clonal Heterogeneity and Tumor Evolution: Past, Present, and the Future. *Cell* **168**, 613-628 (2017).
8. C. Grassberger *et al.*, Patient-Specific Tumor Growth Trajectories Determine Persistent and Resistant Cancer Cell Populations during Treatment with Targeted Therapies. *Cancer Res* **79**, 3776-3788 (2019).

9. N. Wagle *et al.*, Dissecting therapeutic resistance to RAF inhibition in melanoma by tumor genomic profiling. *J Clin Oncol* **29**, 3085-3096 (2011).

10. M. G. O. Fernandes *et al.*, Liquid Biopsy for Disease Monitoring in Non-Small Cell Lung Cancer: The Link between Biology and the Clinic. *Cells* **10**, (2021).

11. C. Karlovich *et al.*, Assessment of EGFR Mutation Status in Matched Plasma and Tumor Tissue of NSCLC Patients from a Phase I Study of Rociletinib (CO-1686). *Clin Cancer Res* **22**, 2386-2395 (2016).

12. C. Gridelli *et al.*, Non-small-cell lung cancer. *Nat Rev Dis Primers* **1**, 15009 (2015).

13. R. S. Herbst, D. Morgensztern, C. Boshoff, The biology and management of non-small cell lung cancer. *Nature* **553**, 446-454 (2018).

14. R. Rosell *et al.*, Erlotinib versus standard chemotherapy as first-line treatment for European patients with advanced EGFR mutation-positive non-small-cell lung cancer (EURTAC): a multicentre, open-label, randomised phase 3 trial. *Lancet Oncol* **13**, 239-246 (2012).

15. M. Reck *et al.*, Erlotinib in advanced non-small cell lung cancer: efficacy and safety findings of the global phase IV Tarceva Lung Cancer Survival Treatment study. *J Thorac Oncol* **5**, 1616-1622 (2010).

16. G. Recondo, F. Facchinetti, K. A. Olaussen, B. Besse, L. Friboulet, Making the first move in EGFR-driven or ALK-driven NSCLC: first-generation or next-generation TKI? *Nat Rev Clin Oncol* **15**, 694-708 (2018).

17. S. M. Lim, N. L. Syn, B. C. Cho, R. A. Soo, Acquired resistance to EGFR targeted therapy in non-small cell lung cancer: Mechanisms and therapeutic strategies. *Cancer Treat Rev* **65**, 1-10 (2018).

18. H. A. Yu *et al.*, Analysis of tumor specimens at the time of acquired resistance to EGFR-TKI therapy in 155 patients with EGFR-mutant lung cancers. *Clin Cancer Res* **19**, 2240-2247 (2013).

19. C. H. Yun *et al.*, The T790M mutation in EGFR kinase causes drug resistance by increasing the affinity for ATP. *Proc Natl Acad Sci U S A* **105**, 2070-2075 (2008).

20. J. A. Engelman *et al.*, MET amplification leads to gefitinib resistance in lung cancer by activating ERBB3 signaling. *Science* **316**, 1039-1043 (2007).

21. K. Takezawa *et al.*, HER2 amplification: a potential mechanism of acquired resistance to EGFR inhibition in EGFR-mutant lung cancers that lack the second-site EGFRT790M mutation. *Cancer Discov* **2**, 922-933 (2012).

22. M. Emamalipour *et al.*, Horizontal Gene Transfer: From Evolutionary Flexibility to Disease Progression. *Front Cell Dev Biol* **8**, 229 (2020).

23. S. A. Melo *et al.*, Cancer exosomes perform cell-independent microRNA biogenesis and promote tumorigenesis. *Cancer Cell* **26**, 707-721 (2014).

24. C. F. Ruivo, B. Adem, M. Silva, S. A. Melo, The Biology of Cancer Exosomes: Insights and New Perspectives. *Cancer Res* **77**, 6480-6488 (2017).

25. F. T. Borges *et al.*, TGF-beta1-containing exosomes from injured epithelial cells activate fibroblasts to initiate tissue regenerative responses and fibrosis. *J Am Soc Nephrol* **24**, 385-392 (2013).

26. C. Kahlert *et al.*, Identification of double-stranded genomic DNA spanning all chromosomes with mutated KRAS and p53 DNA in the serum exosomes of patients with pancreatic cancer. *J Biol Chem* **289**, 3869-3875 (2014).

679 27. S. Wu *et al.*, Intercellular transfer of exosomal wild type EGFR triggers osimertinib
680 resistance in non-small cell lung cancer. *Mol Cancer* **20**, 17 (2021).
681 28. M. Raudenska, J. Gumulec, J. Balvan, M. Masarik, Caveolin-1 in oncogenic metabolic
682 symbiosis. *Int J Cancer* **147**, 1793-1807 (2020).
683 29. K. Simons, D. Toomre, Lipid rafts and signal transduction. *Nat Rev Mol Cell Biol* **1**, 31-
684 39 (2000).
685 30. H. N. Fridolfsson, D. M. Roth, P. A. Insel, H. H. Patel, Regulation of intracellular
686 signaling and function by caveolin. *FASEB J* **28**, 3823-3831 (2014).
687 31. J. Ketteler, D. Klein, Caveolin-1, cancer and therapy resistance. *Int J Cancer* **143**, 2092-
688 2104 (2018).
689 32. C. C. Ho *et al.*, Caveolin-1 expression is significantly associated with drug resistance and
690 poor prognosis in advanced non-small cell lung cancer patients treated with gemcitabine-
691 based chemotherapy. *Lung Cancer* **59**, 105-110 (2008).
692 33. S. H. Yoo *et al.*, Expression of caveolin-1 is associated with poor prognosis of patients
693 with squamous cell carcinoma of the lung. *Lung Cancer* **42**, 195-202 (2003).
694 34. F. Han, J. Zhang, J. Shao, X. Yi, Caveolin-1 promotes an invasive phenotype and predicts
695 poor prognosis in large cell lung carcinoma. *Pathol Res Pract* **210**, 514-520 (2014).
696 35. F. Liu, Z. Shangli, Z. Hu, CAV2 promotes the growth of renal cell carcinoma through the
697 EGFR/PI3K/Akt pathway. *Onco Targets Ther* **11**, 6209-6216 (2018).
698 36. T. Y. Luan *et al.*, Expression of caveolin-1 is correlated with lung adenocarcinoma
699 proliferation, migration, and invasion. *Med Oncol* **32**, 207 (2015).

700 37. Y. Cui *et al.*, Downregulation of caveolin-1 increased EGFR-TKIs sensitivity in lung
701 adenocarcinoma cell line with EGFR mutation. *Biochem Biophys Res Commun* **495**, 733-
702 739 (2018).
703 38. S. C. Wang, M. C. Hung, Nuclear translocation of the epidermal growth factor receptor
704 family membrane tyrosine kinase receptors. *Clin Cancer Res* **15**, 6484-6489 (2009).
705
706

Acknowledgments:

We thank Dr Nuno Alves, i3S, Porto, Portugal and Dr James Di Santo, Institute Pasteur, Paris, France, for kindly gifting the Ilrg2-/-. We thank Dr. Dina Leitão for assistance in the immunohistochemistry staining. Elaboration of figures 1A and 2A was performed using BioRender.com.

Funding:

This research was funded (in part) by FCT - Fundação para a Ciência e a Tecnologia/Ministério da Ciência, Tecnologia e Ensino Superior in the framework of the projects "Financiamento Plurianual de Unidades de I&D, UIBD/04293/2020", "Horizontal transmission of drug resistance: a game changer in the clinical management of cancer patients" (P2020-PTDC/DTP-PIC/2500/2014), and SFRH/BD/115099/2016 (SJN PhD fellowship), and (in part) by Programa Operacional Regional do Norte by European Regional Development Fund under the project "The Porto Comprehensive Cancer Center" with the reference NORTE-01-0145-FEDER-072678 - Consórcio PORTO.CCC – Porto.Comprehensive Cancer Center.

Author contributions:

Conceptualization: SJN, SAM, JLC and JCM

In vitro and *in vivo* experiments: SJN, ARO, JFM, MS, BA

Other methodology: SJN, ARO, JFM, JP, CSM, JCM, PO.

Analysis of results: SJN, ARO, JFM, PO, LP, BC, JP, CSM, JLC, JCM

Selection of clinical samples and analysis of clinical data: AB, VH, MGOF, CSM, JLC, JCM

Funding acquisition: JLC, JCM.

Writing - original draft: SJN, JCM.

Writing – review & editing: all authors

Competing interests:

SAM holds patents in EVs biology that are licensed to Codiak Biosciences. The other authors declare no competing interests.

Data and materials availability:

All data, except for RNASeq raw data, are available in the main text or the supplementary materials. The RNASeq datasets used and/or analyzed during the current study are available from the corresponding author upon request.

Ethics approval and informed consent:

The study was conducted according to the guidelines of the Declaration of Helsinki. Ethical review and approval were waived as the study is in accordance with Article 19 ("DNA Banks and Other Biological Products") of Portuguese Law No. 12/2005 of 26 January ("Personal genetic information and health information"), which states that in the case of using retrospective samples from human origin or in special situations where the consent of the people involved cannot be obtained because of the amount of data or subjects, of their age, or another reason comparable, material and data can be processed but only for purposes of scientific research or epidemiological and statistical data collection.

Animal studies were approved by the national authority Direção Geral de Alimentação e Veterinária (DGAV reference 0421/000/000/2017) and reviewed by the i3S Animal Welfare and

753 Ethics Body (reference 2016/22). All mice were housed under standard housing conditions at the
754 i3S animal facility.